Crystal structure and low-temperature magnetic properties of R_mMIn$_{3m+2}$ compounds (M=Rh or Ir; m=1,2; R=Sm or Gd)

P. G. Pagliuso, J. D. Thompson, M. F. Hundley, J. L. Sarrao, and Z. Fisk*

Los Alamos National Laboratory, Los Alamos, New Mexico 87545
(Received 29 August 2000; published 11 January 2001)

We have synthesized the series of compounds RMIn$_5$ and R_2MIn$_8$ in single crystal form, where $R=$Sm or Gd and $M=$Rh or Ir. These materials form in tetragonal derivatives of the Cu$_3$Au structure RIn$_3$. Measurements of magnetic susceptibility, electrical resistivity, and low-temperature heat capacity are reported. These compounds order antiferromagnetically at low temperature ($T_N<45$ K) and their low-temperature magnetic properties remain nearly unaltered compared to their SmIn$_3$ and GdIn$_3$ cubic relatives. The present data are compared to the magnetic properties of the isostructural (Ce,Nd) (Rh,Ir)In$_5$ and (Ce,Nd)$_2$(Rh,Ir)In$_8$ compounds, and the validity of de Gennes scaling as a function of rare earth in a given structure is discussed.

I. INTRODUCTION

Recently, a new series of R_mMIn$_{3m+2}$ tetragonal variants of the Cu$_3$Au-structure compounds for $M=$Rh or Ir, $m=1,2$; and $R=$light rare earth have become a particularly relevant area of research since the discovery of a new class of heavy-fermion superconductors for some of the Ce-based compounds.[1–3] The R_mMIn$_{3m+2}$ tetragonal structures can be viewed as m layers of RIn$_3$ units stacked sequentially along the c axis with intervening layers of MIn$_2$ (Ref. 4) and unconventional magnetic and superconducting behavior have been reported for CeRhIn$_5$ (Ref. 1) and CeIrIn$_5$.[2] The first one is an antiferromagnet at ambient pressure ($T_N\approx3.8$ K and $\gamma\approx400$ mJ/mol K^2),[1] and presents an unconventional evolution to a superconducting state for $P>P_c\approx16$ kbars where superconductivity sets in at $T_c\approx2$ K. CeIrIn$_5$ shows ambient-pressure heavy-fermion superconductivity at $T_c\approx0.4$ K with a Sommerfeld coefficient of $\gamma\approx720$ mJ/mol K^2.[2] The $m=2$ variants of these Ce-based compounds include an antiferromagnetic ground state ($T_N\approx2.8$ K and $\gamma\approx400$ mJ/mol K^2) for Ce$_2$RhIn$_8$, while Ce$_2$IrIn$_8$ remains a heavy-fermion paramagnet to 50 mK, with no evidence for a phase transition ($\gamma\approx700$ mJ/mol K^2).[3]

It has been suggested that the reduced spatial dimensionality and magnetic anisotropy resulting from the quasi-two-dimensional structure of these compounds may control the nature of their heavy-fermion ground states.[1,3] Furthermore, studies of NdMIn$_5$ and Nd$_2M$In$_8$ analogs for $M=$Rh or Ir suggest that crystal-field effects (CEF's) and related magnetic anisotropy play an important role in the evolution of the magnetic properties within these series.[5] Therefore studies of the magnetic properties through the rare earths for R_mM_nIn$_{3m+2n}$ ($M=$Rh or Ir) appear to be a promising investigation. The Pr-based homologues are nonmagnetic singlet ground-state systems and a detailed CEF analysis of these materials will be given elsewhere.[6]

In the present work, we report magnetic susceptibility, electrical resistivity, and heat-capacity measurements on (Gd,Sm)MIn$_5$ and (Gd,Sm)$_2M$In$_8$ single crystals, for $M=$Rh or Ir. Each orders antiferromagnetically with $T_N\lesssim45$ K. Comparisons to their cubic relative (Gd,Sm)In$_3$ suggest

that the insertion of MIn$_2$ layers along the c axis in (Gd,Sm)MIn$_5$ and (Gd,Sm)$_2M$In$_8$ ($M=$Rh or Ir) only weakly affects the low-temperature magnetic ground state for the tetragonal variants. The data for the Ce and Nd-based homologues are also included to help the discussion.

II. EXPERIMENT

Single crystalline samples of the (Gd,Sm)MIn$_5$ and (Gd,Sm)$_2M$In$_8$ ($M=$Rh or Ir) compounds were grown from the melt in In flux as described previously.[1] Typical crystal sizes were 1×1 cm$\times$several mm. The tetragonal HoCoGa$_5$ ($m=1$) (Ref. 4) and Ho$_2$CoGa$_8$ ($m=2$) (Ref. 7) structure types and phase purity were confirmed by x-ray powder diffraction, and the crystal orientation was determined by the usual Laue method. The lattice parameters a and c for the studied compounds are given in Table I. Lattice constants for the nonmagnetic variants LaMIn$_5$ and La$_2M$In$_8$ are also included for reference. Specific-heat measurements were per-

TABLE I. Experimental parameters for (Gd,Sm)MIn$_5$, (Gd,Sm)$_2M$In$_8$ ($M=$Rh or Ir), and (Gd,Sm)In$_3$.

|	a Å	c Å	T_N K	μ_{eff} μ_B	θ_p K
GdIrIn$_5$	4.622(4)	7.413(8)	42	7.9(1)	≈-64
Gd$_2$IrIn$_8$	4.615(4)	12.034(7)	41	8.2(1)	≈-75
GdRhIn$_5$	4.609(4)	7.444(7)	40	8.0(1)	≈-69
Gd$_2$RhIn$_8$	4.604(4)	12.060(9)	40	7.4(1)	-73
SmIrIn$_5$	4.634(4)	7.446(7)	14.3		
Sm$_2$IrIn$_8$	4.626(4)	12.088(7)	14.2		
SmRhIn$_5$	4.618(4)	7.470(8)	15.0		
Sm$_2$RhIn$_8$	4.621(4)	12.106(9)	15.0		
LaIrIn$_5$	4.710(4)	7.625(6)			
La$_2$IrIn$_8$	4.703(4)	12.314(7)			
LaRhIn$_5$	4.672(4)	7.602(7)			
La$_2$RhIn$_8$	4.699(4)	12.336(7)			
GdIn$_3$	4.6068[a]		≈45[a]	8.2[a]	≈-85[a]
SmIn$_3$	4.6265[a]		≈16[a]		

[a]See Ref. 7.
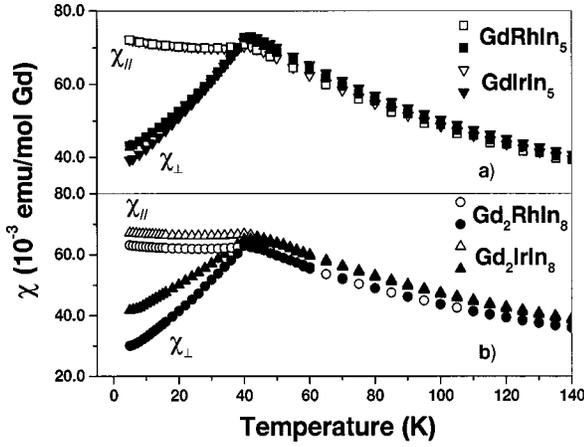
FIG. 1. Temperature dependence of the magnetic susceptibility, for applied field H along the c axis, $\chi_\parallel$ (open symbols), and in the ab plane, $\chi_\perp$ (solid symbols), for $Gd_m M In_{3m+2}$ (M = Rh or Ir) materials (a) for $m=1$ and (b) for $m=2$. The μ_{eff} and θ_p, obtained from Curie-Weiss law fitting for $T>150$ K are given in Table I.

formed in a small-mass calorimeter that employs a quasi-adiabatic thermal relaxation technique.[8] Samples used here ranged from 10 to 30 mg. Magnetization measurements were made in a Quantum Design dc superconducting quantum interference device and electrical resistivity was measured using a low-frequency ac resistance bridge and four-contact configuration.

III. RESULTS

Figures 1 and 2 present the temperature dependence of the magnetic susceptibility, for an applied field H along the c axis, $\chi_\parallel$, and in the ab plane, $\chi_\perp$, for the $Gd_m M In_{3m+2}$ and $Sm_m M In_{3m+2}$ materials, respectively. Each shows antiferromagnetic order, with $T_N < 45$ K. For the Gd-based materials the magnetic susceptibility is significantly anisotropic only below T_N showing a typical anisotropy of an antiferromagnet with an easy axis in the plane. The effective magnetic mo-
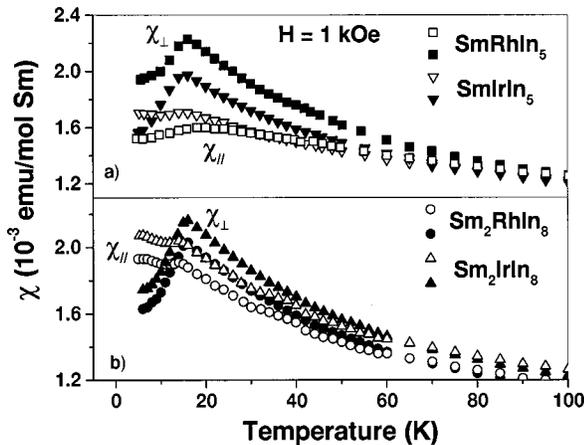

FIG. 2. Temperature dependence of the magnetic susceptibility, for applied field H along the c axis, $\chi_\parallel$ (open symbols), and in the ab plane, $\chi_\perp$ (solid symbols), for $Sm_m M In_{3m+2}$ (M = Rh or Ir) materials (a) for $m=1$ and (b) for $m=2$.
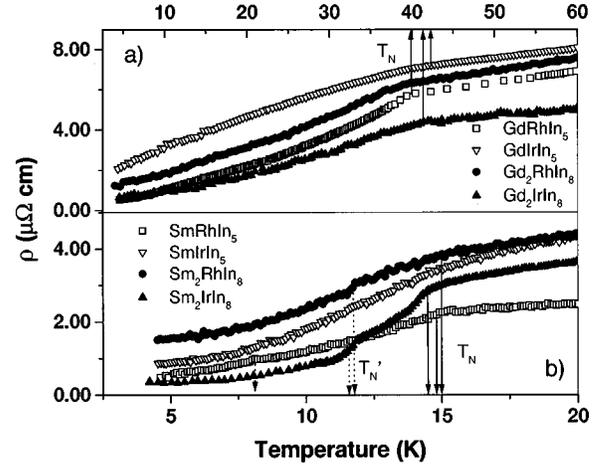

FIG. 3. Temperature dependence of the electrical resistivity for $(Gd,Sm)M In_5$ and $(Gd,Sm)_2 M In_8$ (M = Rh or Ir) single crystals. The solid arrows point out the Néel temperatures for the compounds while the dashed arrows mark possible extra features below T_N.

ment (μ_{eff}) and the paramagnetic Curie-Weiss temperatures (θ_p) obtained from Curie-Weiss law fits for $T>150$ K for the Gd-based compounds are given in Table I. In the Sm-based case, the high-temperature magnetic anisotropy is probably associated with CEF in both ground $J=5/2$ and excited $J=7/2$ multiplet states of the Sm^{3+} ion.[9,10] As typical in Sm-based materials, the high-T behavior of the inverse of magnetic susceptibility does not show a linear temperature dependence due to a Van Vleck contribution (which complicates the extraction of μ_{eff} and θ_p from the data).[9,10]

The temperature dependence of the electrical resistivity for $(Gd,Sm)M In_5$ and $(Gd,Sm)_2 M In_8$ (M = Rh or Ir) single crystals is plotted in Fig. 3. The room-temperature value of the electrical resistivity varies between 20 and 30 $\mu\Omega$ cm and the high-temperature data show a metallic behavior for these compounds. At low temperatures, clear features can be seen at the respective ordering temperatures for all compounds. For the Sm-based homologues extra features also may be present in the data for $T<T_N$ for some of the compounds.

Figure 4 shows the specific heat divided by temperature (a) and the corresponding magnetic entropy (b) in the temperature range $2 \lesssim T \lesssim 20$ K, for $Sm M In_5$ and $Sm_2 M In_8$ (M = Rh or Ir).

To calculate the magnetic entropy, the phonon contribution was estimated from the specific-heat data of $La M In_5$ (Refs. 1 and 2) and $La_2 M In_8$ (Ref. 3) (M = Rh or Ir) and subtracted from the total specific heat of the magnetic compounds. The main peaks in C/T corresponding to the onset of antiferromagnetic order can be seen at $T_N = 14.18$ and 14.30 K for $Sm_2 IrIn_8$ and $SmIrIn_5$, respectively, and at 15.00 K for both $SmRhIn_5$ and $Sm_2 RhIn_8$ [Fig. 4(a)].

The Néel temperatures obtained from the specific-heat data are in very good agreement with the temperatures where the maximum in the magnetic susceptibility occurs (see Fig. 2).

For the $Sm_2 IrIn_8$, the antiferromagnetic transition at 14.18 was found to be a first order transition with a latent heat of ~ 10 J/mol. However, no hysteresis was observed in the re-
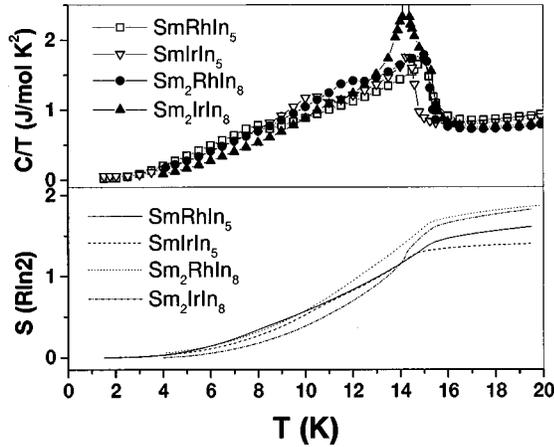
FIG. 4. Specific-heat data divided by temperature (a) and the corresponding magnetic entropy (b) in the temperature range $2 \lesssim T \lesssim 20$ K for $SmM In_5$ and $Sm_2M In_8$ ($M =$ Rh or Ir).

sistivity or magnetic susceptibility measurements as a function of temperature. The magnetic entropy recovered by T_N ranges between 1.4 and $1.8R \ln 2$ [Fig. 4(b)], suggesting that the magnetic order develops in a crystal-field doublet ground state with a nearby doublet excited state. Below T_N, a secondary feature in C_m/T was observed at 11.5, 10.0, 8.0, and 12.0 K for Sm_2IrIn_8, $SmIrIn_5$, $SmRhIn_5$, and Sm_2RhIn_8, respectively [Fig. 4(a)]. These secondary peaks are coincident with features in the resistivity for some of the compounds (see Fig. 3). Similar extra transitions below T_N also have been reported for $SmIn_3$ and they have been interpreted as successive magnetic transitions associated with quadrupolar ordering.[11]

IV. DISCUSSION

The cubic compounds RIn_3 are antiferromagnets with $T_N \lesssim 50$ K (Ref. 9) and their T_N and θ_p values follow de Gennes scaling quite well, with the exception of $CeIn_3$.[9] $NdIn_3$ and $SmIn_3$, whose magnetic order develops in a Γ_8 quartet crystal-field ground state, present additional magnetic transitions below T_N.[11-13] These complex magnetic states with successive magnet ordering arise due to the presence of magnetoelastic effects and both bilinear and quadrupolar exchange interactions.[11-13]

Surprisingly, the insertion of m MIn_2 layers along the c axis in $(Gd,Sm)M In_5$ and $(Gd,Sm)_2M In_8$ ($M =$ Rh or Ir) causes no significant changes in their Néel temperatures, whereas T_N shows a strong variation among the Ce- and Nd-based homologous.[3,5] It has been reported that the magnetization easy axis for $(Ce,Nd)M In_5$ and $(Ce,Nd)_2M In_8$ ($M =$ Rh or Ir) is along the c axis,[3,5] while the present data (see Figs. 1 and 2) suggest an easy axis in the ab plane for the $(Gd,Sm)M In_5$ and $(Gd,Sm)_2M In_8$ ($M =$ Rh or Ir) compounds. As we discuss below, this change in the direction of the magnetic easy axis may be related to a reduction through the rare earths in the competing anisotropic magnetocrystalline and crystal-field effects reported for Ce and Nd.[3,5]

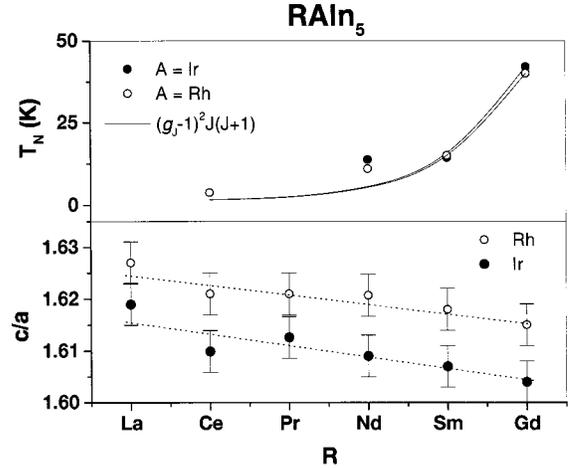In order to discuss the evolution of the magnetic properties of the $RM In_5$ and $R_2M In_8$ ($M =$ Rh or Ir), we plot the

FIG. 5. T_N and c/a values plotted through the rare-earth series for the $RM In_5$ ($M =$ Rh or Ir) compounds. The solid lines are the de Gennes factor $[(g_J^2 - 1)][J(J+1)]$ for ground-state multiplet J of the rare earths normalized by the $GdM In_5$ ($M =$ Rh or Ir) T_N values and the dashed lines are a guide for the eye.

T_N and c/a ratio (see also Table I) for $RM In_5$ ($R =$ Ce,Nd,Sm,Gd; $M =$ Rh,Ir) and $R_2M In_8$ ($R =$ Ce,Nd,Sm,Gd; $M =$ Rh or Ir) in Figs. 5 and 6, respectively. Figure 7 shows the evolution of the Néel temperature for the homologous $RM In_5$ and $R_2M In_8$ ($R =$ Ce,Nd,Gd,Sm; $M =$ Rh or Ir) compounds compared to the their cubic RIn_3 (Ce,Nd,Sm,Gd) relatives.

The solid lines in Figs. 5 and 6 are the de Gennes factor $(g_J^2 - 1)[J(J+1)]$ for ground-state multiplet J through the rare earths. If one normalizes the de Gennes line to the $Gd_m M In_{3m+2}$ ($M =$ Rh or Ir, $m =$ 1,2) T_N values, the Sm-based T_N values sit on the line but the T_N values for the Nd-based and the magnetic Ce-based compounds are above the line (see Figs. 5 and 6). In addition, the evolution of the Néel temperature for the homologous $RM In_5$ and $R_2M In_8$ compounds compared to their cubic RIn_3 relatives, varies by
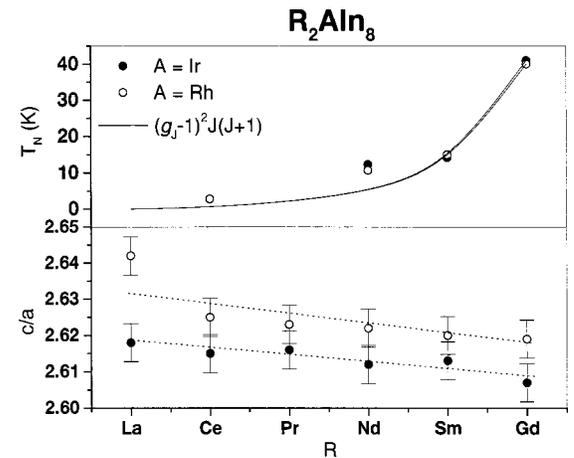

FIG. 6. T_N and c/a values plotted through the rare-earth series for the $R_2M In_8$ ($M =$ Rh or Ir) compounds. The solid lines are the de Gennes factor $[(g_J^2 - 1)][J(J+1)]$ for ground-state multiplet J of the rare earths normalized by the $Gd_2M In_8$ ($M =$ Rh or Ir) T_N values and the dashed lines are a guide for the eye.
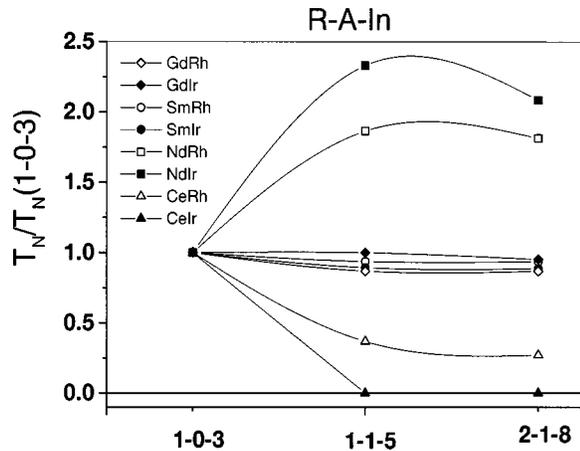
FIG. 7. Evolution of the normalized Néel temperatures for the Gd- and Sm-based compounds. For comparison, data for the homologous Ce- and Nd-based compounds and for cubic $R\text{In}_3$ (R = Ce,Nd,Sm,Gd), are also shown.

less than 10% for R = Gd and Sm while T_N is raised by a factor of 2 for the Nd-based tetragonal variants and is suppressed completely (M = Ir) or to less than 0.5 of the CeIn$_3$ value (M = Rh) for the Ce-based homologous compounds (see Fig. 7).[3,5]

De Gennes scaling[14] does not take into account CEF, Kondo effects, and/or spatial dependence and anisotropic effects in the effective exchange parameter. Some of these effects are clearly present in the Ce-based and Nd-based homologues.[1,3,5] Therefore it is not a surprise that the T_N values for the Ce-based and Nd-based homologues do not follow a de Gennes scaling. Furthermore, our data for Gd- and Sm-based compounds suggest that anisotropic and/or CEF effects may decrease along the rare-earth series. The Sm-based compounds (Sm^{3+} has $J = 5/2$, identical to Ce^{3+}) show smaller ratios $\chi_{easy}/\chi_{\perp easy}$ ranging between 1.05 and 1.30 (see Fig. 2) while these ratios range from 1.20 to greater than 2 for the Ce-based analogues.[3] A possible explanation for this behavior may be related to the systematic decreasing

of c/a ratio through the rare-earth series (see Figs. 5 and 6) which may diminish the tetragonal character of the crystal-electric field and/or the magnetic anisotropy effects in the Sm case. The Gd-based compounds, which are expected to present small CEF due to the S character of the Gd^{3+} (S = 7/2, L = 0) ion, show only slight anisotropy in the magnetic susceptibility above T_N (see Fig. 1) and also small T_N evolution within the $R_m M_n \text{In}_{3m+2n}$ (M = Rh or Ir, m = 1,2; n = 0,1) compounds. Therefore the absence or reduction of Kondo, CEF effects and/or magnetic anisotropy for the $(\text{Gd,Sm})M\text{In}_5$ and $(\text{Gd,Sm})_2M\text{In}_8$ (M = Rh or Ir) compounds may cause their magnetic properties to be roughly the same as their cubic relatives GdIn$_3$ and SmIn$_3$. Further investigation in the evolution of the crystal-field parameters and the character of the magnetic state for $RM\text{In}_5$ and $R_2M\text{In}_8$ including heaviest rare earths (e.g., R = Dy, Er, or Yb) would be valuable in confirming our supposition.

V. CONCLUSIONS

We have reported a new series of Gd- and Sm-based antiferromagnetic ($T_N < 45$ K) compounds. Their low-temperature magnetic properties remain similar to their SmIn$_3$ and GdIn$_3$ cubic relatives. Comparisons among the present data and the magnetic properties of isostructural (Ce,Nd) (Rh,Ir)In$_5$ and (Ce,Nd)$_2$(Rh,Ir)In$_8$ and of de Gennes scaling as a function of rare earth in a given structure suggest that the reduction CEF effects and related magnetic anisotropy through the rare-earth series for the tetragonal variants may cause the magnetic properties of $(\text{Gd,Sm})M\text{In}_5$ $(\text{Gd,Sm})_2M\text{In}_8$ (M = Rh or Ir) and their cubic relatives GdIn$_3$ and SmIn$_3$ to be nearly the same.

*Permanent address: Florida State University, Tallahassee, FL 32306

[1] H. Hegger, C. Petrovic, E.G. Moshopoulou, M.F. Hundley, J.L. Sarrao, Z. Fisk, and J.D. Thompson, Phys. Rev. Lett. **84**, 4986 (2000).

[2] C. Petrovic, R. Movshovich, M. Jaime, M.F. Hundley, J.L. Sarrao, P.G. Pagliuso, Z. Fisk, and J.D. Thompson, Europhys. Lett. (to be published).

[3] J.D. Thompson, R. Movshovich, Z. Fisk, F. Bouquet, N.J. Curro, R.A. Fisher, P.C. Hammel, H. Hegger, M.F. Hundley, M. Jaime, P.G. Pagliuso, C. Petrovic, N.E. Phillips, and J.L. Sarrao, J. Magn. Magn. Mater. (to be published).

[4] E.G. Moshopoulou, Z. Fisk, J.L. Sarrao, and J.D. Thompson, J. Solid State Chem. (to be published).

[5] P.G. Pagliuso, J.D. Thompson, M.F. Hundley, and J.L. Sarrao, Phys. Rev. B **62**, 12 266 (2000).

[6] Pagliuso *et al.* (unpublished).

[7] Ya.M. Kalychak, J. Alloys Compd. **291**, 80 (1999).

[8] R. Bachmann, F.J. DiSalvo, T.H. Geballe, R.L. Greene, R.E. Howard, C.N. King, H.C. Kivisch, K.N. Lee, R.E. Schwall, H.V. Thomas, and R.B. Zubek, Rev. Sci. Instrum. **43**, 205 (1972).

[9] K.H.J. Buschow, H.W. de Wijn, and M. Van Diepen, J. Chem. Phys. **50**, 137 (1969).

[10] T. Tsuchida and W.E. Wallace, J. Chem. Phys. **43**, 3811 (1965).

[11] M. Kasaya, B. Liu, M. Sera, T. Kasuya, D. Endoh, T. Goto, and F. Fujimura, J. Magn. Magn. Mater. **52**, 289 (1985).

[12] M. Amara, R.M. Galéra, P. Morin, T. Verez, and P. Burlet, J. Magn. Magn. Mater. **130**, 127 (1994); M. Amara, R.M. Galéra, P. Morin, J. Voiron, and P. Burlet, *ibid.* **131**, 402 (1994); M. Amara, R.M. Galéra, P. Morin, J. Voiron, and P. Burlet, *ibid.* **140**, 1157 (1994).

[13] A. Czopnik, J. Kowalewski, and M. Hackemer, Phys. Status Solidi A **127**, 243 (1991).

[14] P.G. De Gennes, Compt. Rend. **247**, (1958); P.G. De Gennes, J. Phys. Radium **23**, 510 (1962); B. Coqblin, *The Electronic Structure of Rare-Earth Metal and Alloys: The Magnetic Heavy Rare Earths* (Academic Press, New York, 1977).